Automated Quantification of Volumetric Optic Disc Swelling in Papilledema Using Spectral-Domain Optical Coherence Tomography

Jui-Kai Wang,[1] *Randy H. Kardon,*[2,3] *Mark J. Kupersmith,*[4] *and Mona K. Garvin*[1,3]

Purpose. To develop an automated method for the quantification of volumetric optic disc swelling in papilledema subjects using spectral-domain optical coherence tomography (SD-OCT) and to determine the extent that such volumetric measurements correlate with Frisén scale grades (from fundus photographs) and two-dimensional (2-D) peripapillary retinal nerve fiber layer (RNFL) and total retinal (TR) thickness measurements from SD-OCT.

Methods. A custom image-analysis algorithm was developed to obtain peripapillary circular RNFL thickness, TR thickness, and TR volume measurements from SD-OCT volumes of subjects with papilledema. In addition, peripapillary RNFL thickness measures from the commercially available Zeiss SD-OCT machine were obtained. Expert Frisén scale grades were independently obtained from corresponding fundus photographs.

Results. In 71 SD-OCT scans, the mean (± standard deviation) resulting TR volumes for Frisén scale 0 to scale 4 were 11.36 ± 0.56, 12.53 ± 1.21, 14.42 ± 2.11, 17.48 ± 2.63, and 21.81 ± 3.16 mm^3, respectively. The Spearman's rank correlation coefficient was 0.737. Using 55 eyes with valid Zeiss RNFL measurements, Pearson's correlation coefficient (*r*) between the TR volume and the custom algorithm's TR thickness, the custom algorithm's RNFL thickness, and Zeiss' RNFL thickness was 0.980, 0.929, and 0.946, respectively. Between Zeiss' RNFL and the custom algorithm's RNFL, and the study's TR thickness, *r* was 0.901 and 0.961, respectively.

Conclusions. Volumetric measurements of the degree of disc swelling in subjects with papilledema can be obtained from SD-OCT volumes, with the mean volume appearing to be roughly linearly related to the Frisén scale grade. Using such an approach can provide a more continuous, objective, and robust means for assessing the degree of disc swelling compared with presently available approaches. (*Invest Ophthalmol Vis Sci.* 2012;53:4069–4075) DOI:10.1167/iovs.12-9438

Papilledema, the swelling of the optic nerve head (ONH) due to intracranial hypertension, has been extensively measured by using the six-stage Frisén scale,[1] which involves a subjective assessment of the visual features of the peripapillary retina and the optic disc from fundus photographs. However, use of such a scale is limited by intra- and interobserver variability, the need for specialized clinical expertise, and the ordinal nature of the scale, which is noncontinuous. Therefore, more quantitative methods, on a continuous scale, are needed for assessing the degree of papilledema.

Optical coherence tomography, introduced in 1991 by Huang et al.,[2] enables cross-sectional images of ONH and/or retina to be acquired, and with appropriately developed software tools, quantitative measurements of structures can be obtained. The use of 2-D peripapillary retinal nerve fiber layer (RNFL) measurements from time-domain OCT for the potential assessment of papilledema has been described[3–6]; however, as the ability to differentiate the RNFL from other layers becomes more difficult with increased swelling, such studies either only included cases of mild papilledema[3,5] or observed that the commercial algorithms would frequently fail to segment the RNFL with higher grades of papilledema[6] (Mandel G, et al. *IOVS* 2010;51:ARVO E-Abstract 555). Scott et al.[6] also examined the use of the 2-D peripapillary total retinal (TR) thickness from time-domain OCT scans, finding it to be a more reliable measurement than RNFL thickness for subjects with papilledema, but such measurements were still inherently 2-D in nature and failures of the commercial algorithm still existed, although less.

With the introduction of spectral-domain optical coherence tomography (SD-OCT),[7,8] obtaining volumetric measurements of ophthalmic structures becomes possible. Volumetric measurements may be particularly appealing in cases of optic disc swelling in order to capture the entire extent of the swelling rather than just using measurements from an arbitrary peripapillary circle. However, commercial SD-OCT machines do not yet provide the ability to volumetrically quantify optic disc swelling, as only peripapillary 2-D measurements are available for volumes centered at the ONH. Study authors have previously reported automated three-dimensional (3-D) graph-theoretic methods to simultaneously and optimally segment multiple layers in SD-OCT.[9–13] The purpose of this study is to adapt this novel 3-D segmentation methodology to enable volumetric measurements of optic disc swelling in subjects with papilledema and to determine the extent that these volumetric measurements correlate with Frisén scale grades (from fundus photographs)

From the Departments of [1]Electrical and Computer Engineering and [2]Ophthalmology and Visual Sciences, The University of Iowa, Iowa City, Iowa; the [3]VA Center for the Prevention and Treatment of Visual Loss, Department of Veterans Affairs, Iowa City, Iowa; and the [4]Department of Neuro-Ophthalmology, Roosevelt Hospital and New York Eye and Ear Infirmary, New York, New York.

Supported in part by NIH NEI subcontract R009040554; NIH NEI R01 EY018853, and the Department of Veterans Affairs Rehabilitation Research and Development Division (Iowa City Center for the Prevention and Treatment of Visual Loss and Career Development Award 1IK2RX000728-01; MKG).

Submitted for publication January 5, 2012; revised April 28, 2012; accepted May 8, 2012.

Disclosure: **J.-K. Wang**, None; **R.H. Kardon**, None; **M.J. Kupersmith**, None; **M.K. Garvin**, P

Corresponding author: Mona K. Garvin, 4318 Seamans Center for the Engineering Arts and Sciences, The University of Iowa, Iowa City, IA 52242; mona-garvin@uiowa.edu.

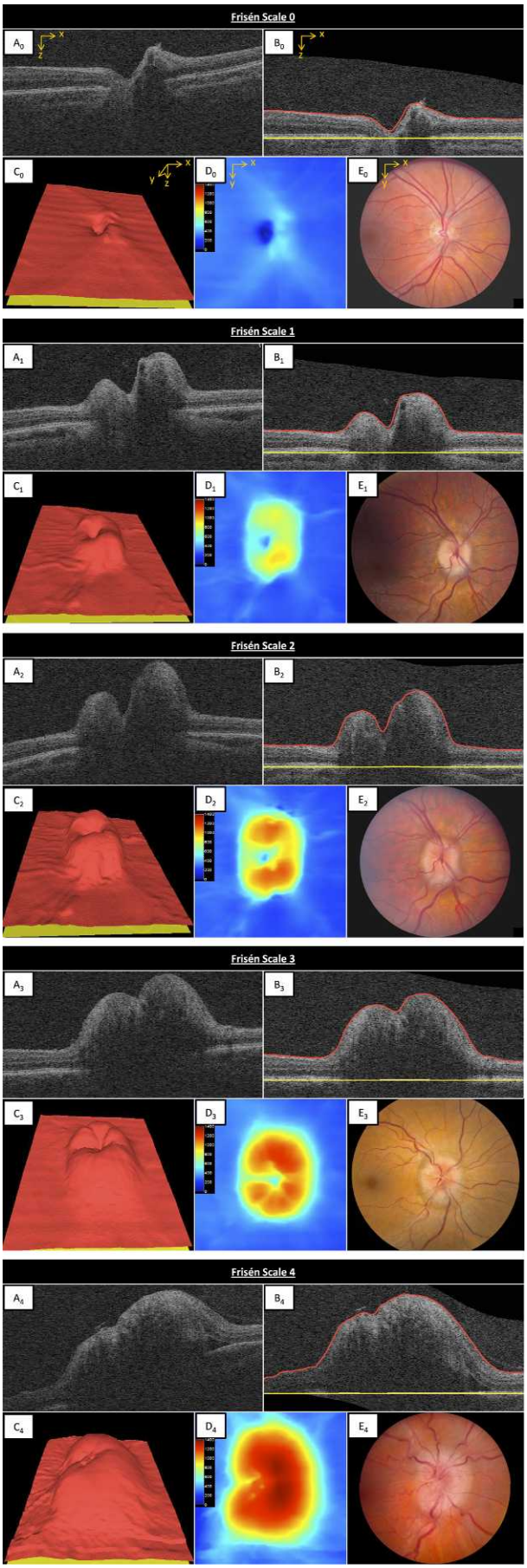

Figure 1. A composite example of papilledema cases of increasing Frisén scales (from scale 0 to scale 4, shown as subscript) with their corresponding retina-optic nerve volumes derived from the 3-D OCT scans. (**A**) A B-scan of the original SD-OCT volume. (**B**) Flattening and layer segmentation, where the red surface is ILM and the yellow surface, which is the reference surface of the flattening, is the lower bounding surface of the RPE complex. (**C**) The 3-D visualization of the entire SD-OCT volume. (**D**) The thickness map between red and yellow surfaces. (**E**) The corresponding fundus image. Note that figures here are displayed using a right-eye orientation/format.

and 2-D peripapillary RNFL and TR thickness measurements from SD-OCT.

Methods

Data Acquisition

In this retrospective study, patients with elevated intracranial pressure and papilledema at initial presentation to the neuro-ophthalmology clinic at the University of Iowa Hospitals and Clinics were included if they had undergone digital fundus photography and OCT (Cirrus; Carl Zeiss Meditec, Dublin, CA) disc scans at the same visit, and all subjects had been imaged at least twice on different dates. Fundus photographs were obtained with a retinal camera (RC50-DX; Topcon, Tokyo, Japan) with a 6-megapixel back (MegaVision, Santa Barbara, CA; 2392×2048 actual image size), which is a full-size (35 mm) CCD sensor (OIS, Sacramento, CA). Each SD-OCT scan had dimensions of $200 \times 200 \times 1024$ voxels ($6 \times 6 \times 2$ mm^3), with a voxel depth of 8 bits in grayscale. SD-OCT scans were excluded if the internal limiting membrane (ILM) or the RPE complex went outside the confines of the volume (*z*-axis) window of the scan. This sometimes occurs with greater severity of papilledema in which it can become more difficult for the OCT scan operator to include the entire height of the elevated optic nerve within the *z*-axis measurement window. The study protocol was approved by the University of Iowa's Institutional Review Board and adhered to the tenets of the Declaration of Helsinki. Because of its retrospective nature, informed consent was not required from subjects.

Expert-Grading of Fundus Photographs Using Frisén Scale

All of the fundus photographs were graded by three independent neuro-ophthalmologists from the University of Iowa using the Frisén scale (from grade 0 to grade 5). The majority outcome was adopted when the original three judgments were not consistent (using a "winner-takes-all" rule). Figures $1E_0$, $1E_1$, $1E_2$, $1E_3$, and $1E_4$ provide example fundus photographs of each grade.

Quantification of Papilledema from SD-OCT Volumes Using Custom Algorithms

The study authors' automated method used a graph-theoretic approach[9,10] to first segment the bounding surfaces of the RNFL and the bounding surfaces of the RPE complex in each SD-OCT volume. A multiresolution scheme was used so that the algorithm first segmented the surfaces in a very low resolution and then repeatedly refined the segmentation results in higher resolutions[14] (Wang J-K, et al. *IOVS* 2011;323:ARVO E-Abstract 2986). As the lower-bounding surface of the RPE complex is not present (undefined) in the region inside the neural canal opening, a thin-plate spline[10,15–17] was then used to interpolate the RPE surface shown at the neural canal border or outside of the ONH opening into the interior region so that an RPE reference surface was completely defined at all *x*-*y* locations in the volume. In addition,

to set up a regular orientation frame for visualization, the curved retinal surface and motion artifact[18,19] of SD-OCT was also modified by realigning the columns of the image until the lower-bounding surface of the RPE complex was flat. Figures $1A_0$, $1A_1$, $1A_2$, $1A_3$, and $1A_4$ show the original SD-OCT volumes of Frisén grades 0, 1, 2, 3, and 4, respectively; and Figures $1B_0$, $1B_1$, $1B_2$, $1B_3$, and $1B_4$ display the segmentation and flattening results (where the red surface is the ILM and the yellow surface is the lower-bounding reference surface of the RPE complex). Based on the layer segmentation results of the custom algorithm three quantitative parameters of SD-OCT volume were measured as described below.

RNFL Peripapillary Circular Thickness. The mean RNFL thickness was first measured around a circle with a radius of 1.73 mm (to match the same settings that Zeiss uses in their commercial machines). Figure 2 provides two examples of this process, where Figures 2A and 2C represent the position of the circular scan in an OCT dataset by the view of the projection image; Figures 2B and 2D are the unwrapped circular OCT scans with the layer segmentation results; and Figure 2E is a B-scan from the same OCT scan of Figure 2C.

TR Peripapillary Circular Thickness. In the same unwrapped circular image as was used for computing the mean RNFL peripapillary circular thickness, the mean TR thickness, between the ILM and the lower bounding surface of RPE complex (the red and yellow surfaces in Figs. 2B, 2D), was also computed.

Total Retinal (TR) Volume. The TR volume was defined by the volumetric region (in mm^3) between the segmented ILM and the lower bounding reference surface of the RPE complex in a complete SD-OCT scan, where Figures $1C_0$, $1C_1$, $1C_2$, $1C_3$, and $1C_4$ are the examples of TR volume visualizations and Figures $1D_0$, $1D_1$, $1D_2$, $1D_3$, and $1D_4$ describe the thickness maps between these two surfaces.

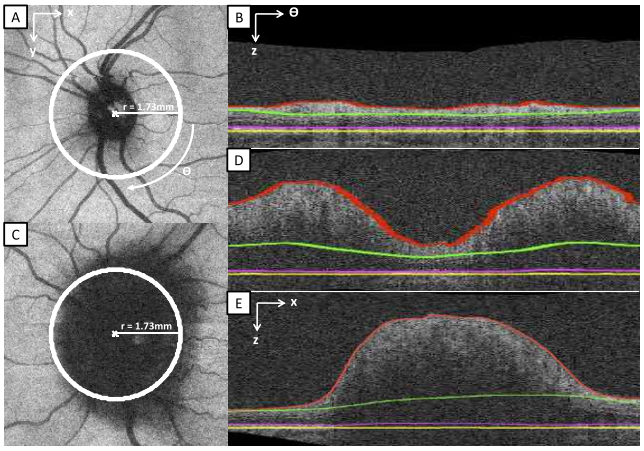

Figure 2. The position of the circular scan (as same as the commercial Zeiss OCT machine) and its layer segmentation in two SD-OCT volumes. (**A**) The position of the circular scan (the white circle) on a normal projection image. (**B**) The 3-D layer segmentation of the unwrapped circular scan of (**A**). (**C**) The position of the circular scan on a projection image with severe papilledema (Frisén scale grade of 4). (**D**) The 3-D layer segmentation of the unwrapped circular scan of (**C**). (**E**) One B-scan of the same SD-OCT volume of (**C**), showing a sagittal cross-section through the center of the optic disc. The segmentation of the ILM border is depicted by the red line; the deeper, outer border of the RNFL by the green line; the photoreceptor boundary by the magenta line; and the retinal pigmented epithelial border by the yellow line. In the region underlying the ONH (**E**), the borders were extrapolated using a spline fit.

Quantification of Papilledema from SD-OCT Volumes Using Zeiss' Algorithm

The mean circular peripapillary RNFL thickness (radius = 1.73 mm) was also measured using the commercial algorithm provided by the SD-OCT scanner (Carl Zeiss Meditec). Any measurements for which the algorithm visually failed were excluded.

Correlation of Volumetric Parameters with 2-D Parameters and "Winner-Take-All" Expert Frisén Grades

TR volume measurements were first correlated to the expert Frisén scale grades and the mean and standard deviation at each grade were computed. Second, TR volume measurements were correlated with each of the 2-D parameters (the study's mean circular RNFL thickness and mean circular TR thickness, and the mean circular RNFL thickness from the Zeiss algorithm). Third, the circular RNFL measurements from the Zeiss algorithm were correlated with the study's circular RNFL measurements and circular total retinal thickness measurements.

Results

Twenty-two patients with papilledema from the University of Iowa were enrolled in the study for which study authors had data from a total of 86 eyes (including right and/or left eyes for different visit dates). Each patient had between two and four separate visit dates (12/22 subjects had two visits, 7/22 had three visits, and 3/22 had four), with the mean (± standard deviation) time interval between visits being 92 (± 80) days. In this original dataset, 5/86 (6%) had Frisén scale 0; 26/86 (30%) had scale 1; 33/86 (38%) had scale 2; 10/86 (12%) had scale 3; and 12/86 (14%) had scale 4. In defining these majority-rule grades, all three experts provided the same grade in 40/86 (47%) cases; one expert disagreed with the other two by one scale grade in 36/86 (42%) cases; one expert disagreed with the other two by two scale grades in 6/86 (7%) cases; and all three experts disagreed in 4/86 (5%) cases.

For all analyses involving SD-OCT–based TR volume measurements, 15/86 (17%) of SD-OCT volumes were excluded because the scans recorded did not contain the complete depth of the disc tissue from the ILM to the RPE within the *z*-plane of the imaging window due to operator error. Summaries of the data inclusion and exclusion results are shown in Table 1 and Figure 3. Of the remaining 71 volumes measured, 5 (7%) had Frisén scale 0; 25 (35%) had scale 1; 28 (39%) had scale 2; 8 (11%) had scale 3; and 5 (7%) had scale 4. There were no cases of Frisén scale 5, the severest grade of papilledema, in this dataset.

The mean (± standard deviation) resulting volumes for scale 0 to scale 4 were 11.36 ± 0.56, 12.53 ± 1.21, 14.42 ± 2.11, 17.48 ± 2.63, and 21.81 ± 3.16 mm^3, respectively (Fig. 4). The Spearman rank coefficient between the TR volume and Frisén scale was 0.737 ($P < 0.0001$) (Table 2).

In the subsequent analyses involving the mean RNFL circular thickness from the Zeiss algorithm, 27/86 eyes from the original dataset needed to be excluded because of failures of the proprietary Zeiss algorithm for segmenting the RNFL. Four additional eyes were excluded using the original exclusion criteria (incomplete ILM or RPE included within the volume acquired within *z*-axis window of the OCT scan), thus leaving 55 eyes in the subsequent analyses, comparing the TR volume with the thickness of the peripapillary RNFL (Table 1 and Fig. 3). Using these 55 eyes, the computed Pearson's correlation coefficients (r) between the TR volume measurements and the mean circular TR thickness, the mean circular RNFL thickness (using the current study's custom algorithm),

Table 1. Summary of Inclusion and Exclusion Rates for the Volumetric Analysis and SD-OCT Scanner RNFL Analyses of SD-OCT Volumes

		3-D SD-OCT Scan Acquisition*			SD-OCT Scanner Analysis†			Subsequent Analyses‡		
Frisén Scale	**Sum**	**Include**	**Exclude**	**Exclude Rate**	**Include**	**Exclude**	**Exclude Rate**	**Include**	**Exclude**	**Exclude Rate**
0	5	5	0	0%	5	0	0%	5	0	0%
1	26	25	1	4%	24	2	8%	23	3	12%
2	33	28	5	15%	24	9	27%	21	12	36%
3	10	8	2	20%	5	5	50%	5	5	50%
4	12	5	7	58%	1	11	92%	1	11	92%
Total	86	71	15	17%	59	27	31%	55	31	36%

* In this study, the 3-D segmentation approach needs a complete 3-D volume acquired within the confines of the *z*-axis window, so the reason for the 3-D OCT data exclusions was that these scans were incomplete, meaning that some parts of the ILM or RPE were cut off during acquisition of the entire SD-OCT volume, due to operator error.

† The SD-OCT scanner algorithm (Zeiss Cirrus) for segmenting the RNFL fails more frequently with greater severity scale of papilledema due to the distortion of tissue boundaries used to find the borders of the RNFL.

‡ In the subsequent analyses, the data were the intersection of * and †, which means valid eyes in this dataset were those in which the propriety Zeiss algorithm for determining RNFL thickness did not fail and those where the SD-OCT volume scans were not truncated during acquisition.

and the mean circular RNFL thickness (using the Zeiss algorithm) measurements were 0.980 ($P < 0.0001$), 0.929 ($P < 0.0001$), and 0.946 ($P < 0.0001$), respectively (Fig. 5A, Table 3). The computed Pearson's correlation coefficient (r) between the mean circular Zeiss RNFL thickness measurements and the current custom algorithm's corresponding circular RNFL thickness measurements and mean circular peripapillary TR thickness measurements were 0.901 ($P = 0.0001$) and 0.961 ($P < 0.0001$), respectively (Fig. 5B, Table 3).

Discussion

To support consistent layer segmentation results, the automated graph-theoretic approach of the current study presently requires that the input SD-OCT scans must contain the complete ILM and RPE complex width within the boundary of the *z*-axis window on the scan. The reason is that the algorithm of the current study calculates the global optimal surfaces (based on the cost functions) in the SD-OCT volume, but the result would not be as accurate if some parts of layer information are missing. Therefore, 15 scans out of a total of 86 were not analyzed because they did not have complete ILM and RPE information (Table 1). Since this was a retrospective study, the OCT technician did not have instructions to verify that the entire boundary of the optic disc from the ILM to the RPE layers be included in the scan, which can sometimes be difficult to achieve without careful attention during scan acquisition in cases of the most severe grades of papilledema. Study authors are currently developing interpolation algorithms that will overcome instances in which the 3-D scans are truncated, where the top of the elevated disc may have been excluded during the scan (Wang J-K, et al. *IOVS* 2012; 373:ARVO E-Abstract 3922).

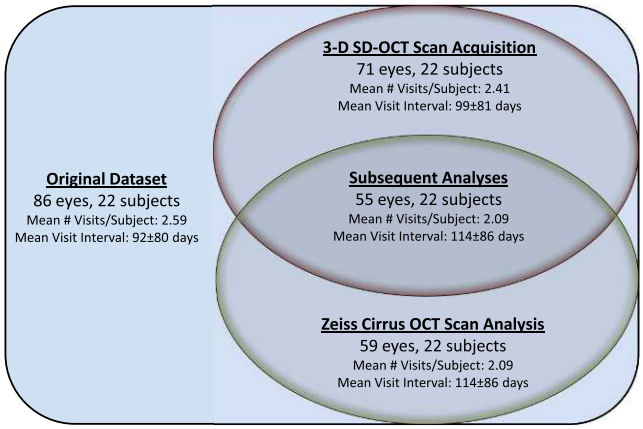

Figure 3. A Venn diagram showing the data used in the study's experiments. The original dataset included 86 SD-OCT volumes and fundus photographs from 22 subjects. The exclusion of 15 volumetric scans (due to an incompletely acquired ILM or RPE in the confines of the *z*-axis window) resulted in 71 volumetric SD-OCT volumes and fundus photographs from 22 subjects (indicated in red). This dataset was used for the first part of the study analyses. From the original dataset, the exclusion of 27 SD-OCT volumes due to the obvious failure of the SD-OCT scanner RNFL algorithm resulted in 59 volumetric SD-OCT volumes and fundus photographs from 22 subjects (indicated in green). This dataset was not directly used in the study analyses. The intersection of these two datasets (labeled "Subsequent Analyses") resulted in 55 SD-OCT volumes and fundus photographs from 22 subjects. This dataset was used for the remaining analyses. For each dataset, the mean number of visits per subject and mean time interval (± standard deviation) between visits is also shown.

Figure 4 demonstrates that the mean TR volume increased incrementally from low Frisén scale grade to high. In addition, the Spearman rank correlation between the TR volumetric measurement and Frisén scale was high (0.737). This high correlation helps to validate that the continuous OCT volumetric measurement provides a quantitative alternative to the ordinal Frisén scale grade. A continuous scale measurement could provide a potential advantage for determining small changes over time in patients being treated with papilledema and followed over time. The objectivity of such continuous measurements is also an important advantage, considering the observed variability of the scale grades between the three experts (all agreeing on the scale grade only 47% [40/86] of the time).

As Scott et al.[6] and others (Mandel G, et al. *IOVS* 2010;51:ARVO E-Abstract 555) mentioned, the commercial Zeiss time- and spectral-domain OCT machines were not specifically designed for papilledema to assess the RNFL thickness, so the commercial algorithm frequently failed with severe papilledema (e.g., 92% of the grade 4 cases needed to be excluded), whereas the approach reported here to measure the total volume of the retina and disc was shown to be more robust. In addition, the total retinal-optic nerve volume was highly correlated with the peripapillary measures of RNFL and TR thickness in scans where the commercial algorithm did not fail (Fig. 5A), further validating its use as a continuous measure of severity of papilledema. The 3-D segmentation approach used here for determining volume and thickness of retinal

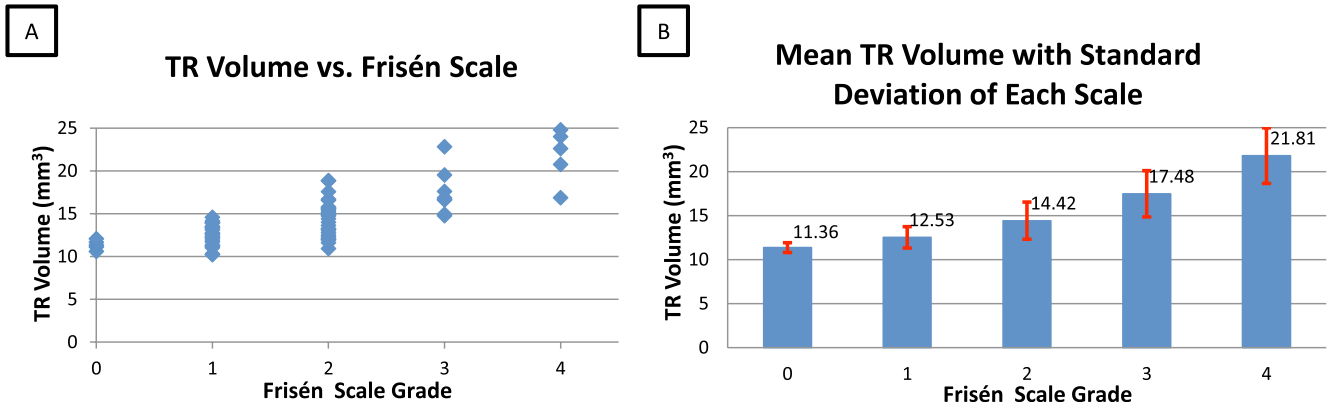

Figure 4. Papilledema grading differences in 71 eyes. **(A)** The scatter of TR volume versus Frisén scale. **(B)** The mean TR volumes with standard deviations of each Frisén scale.

layers (i.e., peripapillary RNFL and TR thickness within a circular region of interest) has distinct advantages over the commonly used 2-D segmentation approaches that are performed on individual OCT B-scans using internal software algorithms that are proprietary to a particular instrument manufacturer. 2-D algorithms are more subject to perturbations from local artifacts, which can cause them to fail, as they do not take advantage of image features contributed by contiguous regions of interest in all neighboring planes, as do the 3-D segmentation and volume determinations reported in this study.

In this study, besides deriving the entire retina-disc volume, study authors were also able to segment the whole RNFL and derive its volume within the entire SD-OCT image acquired. In doing so, the 3-D information could be used to locate the 2-D RNFL and TR thickness in the peripapillary region corresponding to the location of the standard circular scan. This resulted in a more dependable result than could be obtained with the instrument's proprietary 2-D algorithm. Figure 2E is a B-scan with layer segmentations from the same SD-OCT volume as Figure 2C, where it can be seen that the layers were segmented reasonably well in the 3-D domain. The border of the RNFL facing the outer retina becomes more ambiguous and difficult to define in the regions underlying the most edematous areas surrounding the swollen nerve, owing to the attenuation of the OCT signal in deeper layers and distortion of retinal architecture by severe edema. It appears that the rendering of the RNFL volume from 3-D segmentation using all regions of the scan, even those further from the disc, provides a more stable foundation upon which to derive the associated circular peripapillary 2-D RNFL thickness. The advantage of the 3-D segmentation can be seen in Table 1, showing a much lower failure rate for retinal-disc volume, peripapillary RNFL, and peripapillary retinal thickness compared with the standard 2-D RNFL segmentation used by OCT manufacturers.

Table 2. Distribution, Mean Volume and Volume Standard Deviation of Included SD-OCT Scans for Each Grade of Papilledema Severity Using the Frisén Scale in 71 Eyes

Frisén Scale	Number of Eyes	Mean Volume	Standard Deviation
0	5	11.36	0.560
1	25	12.53	1.214
2	28	14.42	2.113
3	8	17.48	2.629
4	5	21.81	3.159
Spearman's rank correlation coefficient		$r = 0.737$	
Significance level		$P < 0.0001$	
95% confidence interval		(0.608, 0.828)	
Total valid eyes		71	

However, using 3-D information to find the RNFL thickness in the 2-D corresponding unwrapped OCT scan is not a perfect solution. As mentioned, in some severe papilledema cases, the RNFL is almost indistinguishable from the other retinal layers. And, due to poor light penetration through the swelling, the RPE/BM neural canal border is not readily seen. In this situation, the derivation of the mean TR thickness in the circular peripapillary region would be a very good alternative, because the RPE complex is usually much more distinct and can be more consistently determined than the boundary surface of RNFL facing the outer retina. The peripapillary TR thickness also has the potential advantage over the TR volume in its ability to be defined even when the top of the nerve head has been truncated in the volumetric scan. Even though the mean TR thickness measurement seems more robust than the mean RNFL thickness in the peripapillary retina, an important limitation still exists in both of these measurements. Both measurements estimate the retinal thickness for different layers in the unwrapped circular OCT scan, but the estimation results would be affected adversely if inaccurate layer segmentations derived from 3-D information coincidentally occurred at the coordinates of the circular scan (Figs. 2A, 2C).

One important future extension of this work will be in identifying appropriate volumetric features that can help differentiate papilledema from other causes of optic disc swelling and pseudopapilledema, which the present work does not address. The best features may very well be "regional" in nature (e.g., total volume outside the ONH region versus inside the ONH region, quadrant volumes, and regional shape parameters). Importantly, the true 3-D segmentation approach reported in this work provides the flexibility to easily compute such regional volumetric features for use in future studies. It may also prove important to combine features from fundus photographs to build upon the recent work of others, such as Carta et al.,[20] that have focused on using fundus features in a classification-based approach to differentiate true optic disc swelling from pseudoedema.

Overall, intuitively, volumetric estimation is a straightforward approach for measuring papilledema, because papilledema manifests as swelling of the peripapillary retina and optic nerve. Based on this study's segmentation results, the total retinal-optic nerve volume (between the red and yellow surfaces in Fig. 1) was not difficult to compute; and the 3-D visualization and the thickness map (shown in Figs. 1C and 1D,

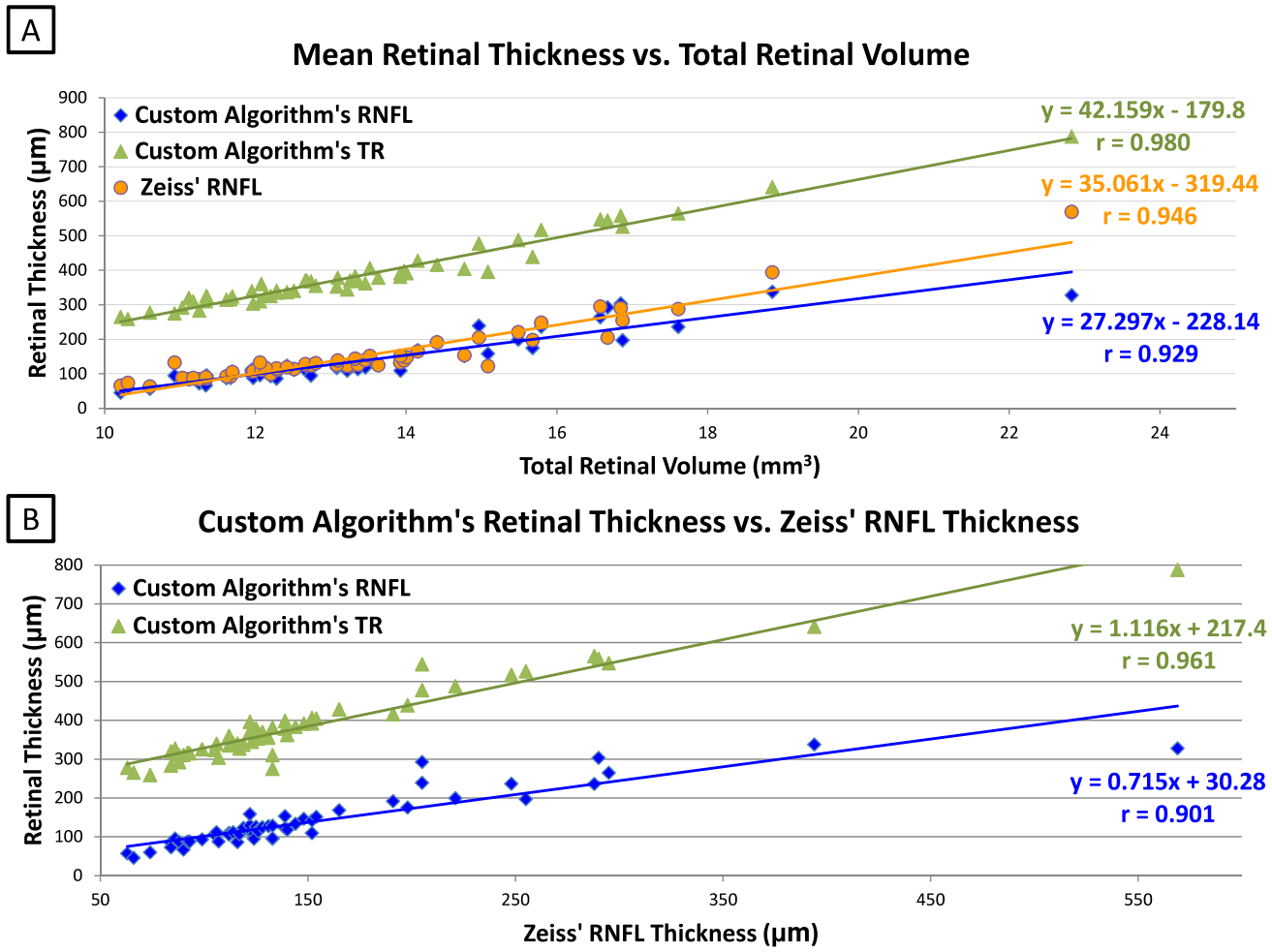

Figure 5. Measurement correlations between total retinal-disc volume and peripapillary RNFL and TR thickness in 55 valid eyes.* (**A**) Compares the study's RNFL, Zeiss RNFL, and the study's TR thickness measurements with the TR volume measurement. (**B**) Compares the relationship between study approaches (including RNFL and TR thickness) and the Zeiss algorithm. * Valid eyes included were those in which the proprietary Zeiss algorithm for determining RNFL thickness did not fail and those where the volume scans were not truncated during acquisition (labeled "Subsequent Analyses" in Table 1 and Fig. 3). In addition to the Zeiss algorithm for determining RNFL, the TR volume, peripapillary retinal thickness (all retinal layers included), and peripapillary RNFL were determined using internally developed algorithms.

respectively) are also useful to help diagnose and follow papilledema over time. Since the volumetric measurement is based on a 3-D approach, more image information is available in a voxel format compared with the pixel format of a 2-D thickness measurement. Also, the entire 3-D retinal volume would be expected to be more resistant to local artifacts or isolated algorithm perturbations affected by a low signal-to-noise ratio in areas of the OCT scan. Future studies will focus on shape features of the rendered volume and internal structural features of the optic disc and surrounding retina, which may provide a means for differentiating causes of optic disc edema and small changes over time. In summary, the total retinal-optic nerve volume rendered from 3-D OCT scans appears to provide an excellent continuous scale measurement of optic disc edema and changes over time.

References

1. Frisén L. Swelling of the optic nerve head: a staging scheme. *J Neurol Neurosurg Psychiatry.* 1982;4513–18.
2. Huang D, Swanson EA, Lin CP, et al. Optical coherence tomography. *Science*. 1991;254:1178–1181.

Table 3. Pearson's Correlation Coefficients in 55 Valid Eyes

Pearson's Correlation Coefficients	*r*	95% Confidence Interval
TR volume vs. Zeiss RNFL*	0.946	(0.909, 0.968)
TR volume vs. RNFL*	0.929	(0.881, 0.958)
TR volume vs. TR thickness*	0.980	(0.966, 0.988)
Zeiss RNFL vs. RNFL†	0.901	(0.836, 0.941)
Zeiss RNFL vs. TR thickness†	0.961	(0.934, 0.977)

Valid eyes included were those in which the proprietary Zeiss algorithm for determining RNFL thickness did not fail and those where the volume scans were not truncated during acquisition (labeled "Subsequent Analyses" in Table 1 and Figure 3). In addition to the Zeiss algorithm for determining RNFL, the TR volume, peripapillary retinal thickness (all retinal layers included), and peripapillary retinal nerve fiber layer (RNFL) were determined using internally developed algorithms (see Figure 5).

* TR volume and the study's retinal thickness measurements ($P < 0.0001$ for all correlations).

† Zeiss RNFL thickness and the custom algorithm's quantitative measurements ($P < 0.00001$ for all correlations).

3. Karam EZ, Hedges TR. Optical coherence tomography of the retinal nerve fibre layer in mild papilloedema and pseudopapilloedema. *Br J Ophthalmol*. 2005;89:294–298.
4. Savini G, Bellusci C, Carbonelli M, et al. Detection and quantification of retinal nerve fiber layer thickness in optic disc edema using stratus OCT. *Arch Ophthalmol*. 2006;124: 1111–1117.
5. Rebolleda G, Muñoz-Negrete FJ. Follow-up of mild papilledema in idiopathic intracranial hypertension with optical coherence tomography. *Invest Ophthalmol Vis Sci*. 2009;50:5197–5200.
6. Scott CJ, Kardon RH, Lee AG, Frisén L, Wall M. Diagnosis and grading of papilledema in patients with raised intracranial pressure using optical coherence tomography vs clinical expert assessment using a clinical staging scale. *Arch Ophthalmol*. 2010;128:705–711.
7. Wojtkowski M, Leitgeb R, Kowalczyk A, Bajraszewski T, Fercher AF. In vivo human retinal imaging by Fourier domain optical coherence tomography. *J Biomed Opt*. 2002;7:457–463.
8. Wojtkowski M, Bajraszewski T, Gorczyńska I, et al. Ophthalmic imaging by spectral optical coherence tomography. *Am J Ophthalmol*. 2004;138:412–419.
9. Li K, Wu X, Chen DZ, Sonka M. Optimal surface segmentation in volumetric images–a graph-theoretic approach. *IEEE Trans Pattern Anal Mach Intell*. 2006;28:119–134.
10. Garvin MK, Abràmoff MD, Wu X, et al. Automated 3-D intraretinal layer segmentation of macular spectral-domain optical coherence tomography images. *IEEE Trans Med Imaging*. 2009;28:1436–1447.
11. Antony BJ, Abramoff MD, Lee K, et al. Automated 3D segmentation of intraretinal layers from optic nerve head optical coherence tomography images. In: Molthen RC, Weaver JB, eds. *Proceedings of SPIE Medical Imaging 2010: Biomedical Applications in Molecular, Structural, and Functional Imaging*. Vol. 7626. 2010;76260U-1–76260U-12.
12. Lee K, Abramoff MD, Niemeijer M, Garvin MK, Sonka M. 3-D segmentation of retinal blood vessels in spectral-domain OCT volumes of the optic nerve head. In: Molthen RC, Weaver JB, eds. *Proceedings of SPIE Medical Imaging 2010: Biomedical Applications in Molecular, Structural, and Functional Imaging*. Vol. 7626. 2010;76260V-1–76260V-8.
13. Lee K, Abràmoff M, Sonka M, Garvin MK. Automated segmentation of intraretinal layers from spectral-domain macular OCT: reproducibility of layer thickness measurements. In: Weaver JB, Molthen RC, eds. *Proceedings of SPIE Medical Imaging 2011: Biomedical Applications in Molecular, Structural and Functional Imaging*. Vol. 7965. 2011; 796523-1–796523-8.
14. Lee K, Niemeijer M, Garvin MK, et al. Segmentation of the optic disc in 3-D OCT scans of the optic nerve head. *IEEE Trans Med Imaging*. 2010;29:159–168.
15. Duchon J. Splines minimizing rotation-invariant semi-norms in Sobolev spaces. In: Schempp W, Zeller K, eds. *Constructive Theory of Functions of Several Variables: Lecture Notes in Mathematics*. 1977;571/1977:85–100.
16. Bookstein FL. Principal warps: thin-plate splines and the decomposition of deformations. *IEEE Trans Pattern Anal Mach Intell*. 1989;11:567–585.
17. Powell MJD. The uniform convergence of thin plate spline interpolation in two dimensions. *Numerische Mathematik*. 1994;68:107–128.
18. Ricco S, Chen M, Ishikawa H, Wollstein G, Schuman J. Correcting motion artifacts in retinal spectral domain optical coherence tomography via image registration. In: Yang G-Z, Hawkes D, Rueckert D, Noble A, and Taylor C, eds. *Medical Image Computing and Computer-Assisted Intervention – MICCAI 2009: Lecture Notes in Computer Science*. 2009; 5761/2009:100–107.
19. Xu J, Ishikawa H, Wollstein G, Schuman JS. 3D OCT eye movement correction based on particle filtering. *Conf Proc IEEE Eng Med Biol Soc*. 2010;2010:53–56.
20. Carta A, Favilla S, Prato M, et al. Accuracy of funduscopy to identify true edema versus pseudoedema of the optic disc. *Invest Ophthalmol Vis Sci*. 2012;53;1–6.